INVESTIGATING QUADRUPOLE BANDS IN ^{180}Hf AND ^{182}W*

Polytimos Vasileiou, Theo J. Mertzimekis

Department of Physics, National & Kapodistrian University of Athens
Zografou Campus, 15784, Greece

Dennis Bonatsos

Institute of Nuclear and Particle Physics
National Centre for Scientific Research "Demokritos"
15310, Aghia Paraskevi, Greece

Received 13 December 2024, accepted 13 January 2025, published online 10 April 2025

The structure of the low-lying quadrupole bands in ^{180}Hf and ^{182}W is investigated with the use of a microscopically derived IBM-1 Hamiltonian. For each isotope, a potential energy curve is constructed from self-consistent mean-field calculations, employing a Skyrme energy density functional. The fermionic potential energy curve is subsequently mapped onto the corresponding bosonic one, thus leading to the derivation of the IBM-1 Hamiltonian parameters. These parameters are then used as inputs for the calculation of energy spectra and B(E2) transition strengths for the ground state and γ bands in the examined isotopes. The results are compared to experimental data, showing an overall good agreement. Potential future applications of this mapping method are also discussed.

DOI:10.5506/APhysPolBSupp.18.2-A23

1. Introduction

Triaxiality [1–3] in atomic nuclei has been a long-standing puzzle in nuclear structure, its nature and origins being the subject of numerous experimental as well as theoretical studies over the years. The topic has attracted considerable attention in recent years, with studies suggesting the presence of triaxiality over extended regions of the nuclear chart [4–6].

In our recent paper [7], we proposed a method of incorporating triaxiality into the classical limit of the interacting-boson-model-1 (IBM-1) [8–10], where only one- and two-body terms were considered. To that end, the proxy-SU(3) [11–13] symmetry was employed. Fermionic proxy-SU(3)

* Presented at the 57$^{\text{th}}$ Zakopane Conference on Nuclear Physics, *Extremes of the Nuclear Landscape*, Zakopane, Poland, 25 August–1 September, 2024.

highest weight (h.w.) irreps were used to derive a γ-deformation value for the isotopes under examination, which was subsequently incorporated into the IBM-1 potential energy curve (PEC). Resembling the method described in [14–16], a mapping was performed between the IBM-1 PEC and a corresponding PEC resulting from self-consistent mean-field (SCMF) calculations [17], to derive the IBM-1 Hamiltonian parameters. These microscopically derived parameters were then used as inputs for the calculation of energy spectra and B(E2) transition strengths for the even–even Hf and W isotopes under consideration.

It was shown that the inclusion of this γ deformation, of microscopic origin, derived in a parameter-free way through the use of proxy-SU(3) h.w. irreps, as dictated by the Pauli principle and the short-range nucleon–nucleon interaction, led to significantly improved results compared to axially-symmetric calculations, in good agreement with experiment.

In this contribution, we intend to give a brief outline of the theoretical method implemented in our calculations, and feature selected results for the cases of ^{180}Hf and ^{182}W. For the interested reader, the full scope of the work, along with an in-depth discussion of the results, can be found in [7].

2. Theoretical procedure

For the construction of the microscopic PECs, SCMF calculations are performed on a two-dimensional grid of the r–z plane, with a constraint been placed on the quadrupole deformation variable, β. The axial Hartree–Fock+Bardeen–Cooper–Schrieffer (HF+BCS) code SkyAx [17] is employed, utilizing the SV-bas [18] Skyrme energy density functional (EDF), along with a density-dependent δ-force used for the pairing (see [7, 17] for more details).

Regarding the IBM-1 PECs, the extended consistent Q formalism (ECQF) is employed to write the Hamiltonian as

$$H(\zeta,\chi) = c\left[(1-\zeta)\hat{n}_d - \frac{\zeta}{4N_B}\hat{Q}^\chi\cdot\hat{Q}^\chi\right], \tag{1}$$

where N_B is the number of valence bosons, $\hat{n}_d$ is the number operator for quadrupole bosons, $\hat{Q}^\chi = (s^\dagger\tilde{d}+d^\dagger s)+\chi(d^\dagger\tilde{d})^{(2)}$ is the quadrupole operator, and c is a scaling factor.

The corresponding IBM-1 energy surface, $E_{\rm IBM}(\bar{\beta},\gamma)$ is derived by using the coherent state formalism [8–10] of the IBM, as [19]

$$\begin{aligned} E_{\rm IBM}\left(\bar{\beta},\gamma\right) &= \frac{cN_B\bar{\beta}^2}{1+\bar{\beta}^2}\left[(1-\zeta)-\left(\chi^2+1\right)\frac{\zeta}{4N_B}\right]-\frac{5c\zeta}{4\left(1+\bar{\beta}^2\right)} \\ &\quad -\frac{c\zeta(N_B-1)}{4\left(1+\bar{\beta}^2\right)^2}\times\left[4\bar{\beta}^2-4\sqrt{\frac{2}{7}}\chi\bar{\beta}^3\cos 3\gamma+\frac{2}{7}\chi^2\bar{\beta}^4\right], \end{aligned} \tag{2}$$

where $C_\beta = \bar{\beta}/\beta$ is a proportionality coefficient relating the bosonic ($\bar{\beta}$) and fermionic (β) quadrupole deformation variables. Equation (2) relates the structural parameters (χ, ζ) of (1) with the (β, γ) classical coordinates linked to the Bohr geometrical variables. More specifically, ζ is related to the axial quadrupole deformation parameter, β, while χ is associated with the triaxiality parameter, γ.

Finally, the proxy-SU(3) approximation to the shell model is employed to derive an intrinsic γ-deformation value [20, 21]

$$\gamma_{\rm s} = \arctan\left(\frac{\sqrt{3}(\mu+1)}{2\lambda+\mu+3}\right), \tag{3}$$

where (λ, μ) are the Elliott labels of the proxy-SU(3) h.w. irreps. By incorporating (3) into (2), we obtain the IBM-1 PEC. Its parameters, namely $(\chi, \zeta, c, C_\beta)$ are determined through a mapping onto the SCMF PEC, where the aim is to achieve an optimal reproduction of the overall shape and curvature of the latter, up to a few MeV from its absolute minimum (Fig. 1). These parameters are then used as inputs for the calculation of ground-state (g.s.) and γ-band energy levels, carried out with the help of the IBAR [22] code. In the end, a rescaling of the predicted γ-band energy levels to their respective experimental bandheads is performed. This is associated with different mass coefficients, corresponding to varying moments of inertia between the g.s. and γ bands (see *e.g.* [23–25]).

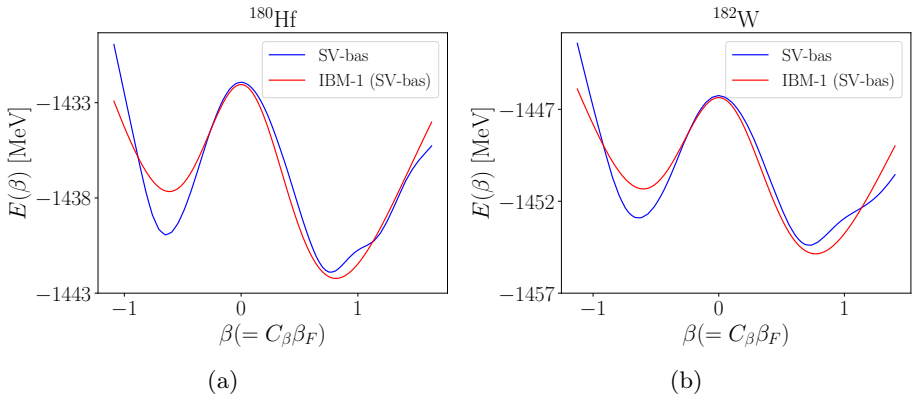

Fig. 1. (Color online) SV-bas EDF potential energy curves (blue/black) *versus* the corresponding IBM-1 ones (red/gray) for (a) ^{180}Hf and (b) ^{182}W.

3. Results and discussion

As it can be seen from Fig. 2, our calculations are in very good agreement with experimental data for the ground-state band energy levels of ^{180}Hf (a) and ^{182}W (b), even as one moves on to higher spins ($J \geq 6_1^+$). A good agreement is also observed for the members of the γ bands, formed by the 2_2^+, 3_1^+, 4_2^+, ..., 9_1^+ states.

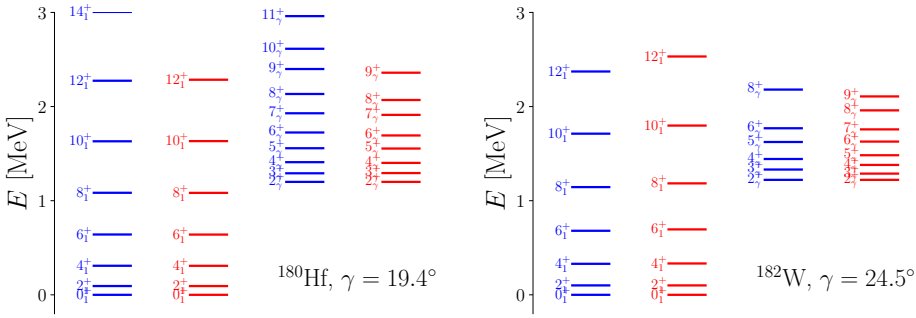

(a) (b)

Fig. 2. (Color online) Experimental (blue/black) *versus* calculated (red/gray) g.s. and γ-band energy levels for (a) ^{180}Hf and (b) ^{182}W.

Table 1. Experimental *versus* calculated $B(\mathrm{E2}; J \to J-2)$ values for ^{180}Hf and ^{182}W. Literature data obtained from [26–28].

Isotope	Transition	$B(\mathrm{E2})$ [W.u.] (Exp.)	$B(\mathrm{E2})$ [W.u.] (Th.)
^{180}Hf	$2_1^+ \to 0_1^+$	155(2)	183.18
	$4_1^+ \to 2_1^+$	234^{+28}_{-23}	260.01
	$6_1^+ \to 4_1^+$	225(16)	282.60
	$8_1^+ \to 6_1^+$	245(13)	289.35
^{182}W	$2_1^+ \to 0_1^+$	134.6(14)	162.40
	$4_1^+ \to 2_1^+$	196(10)	229.48
	$6_1^+ \to 4_1^+$	201(22)	247.63
	$8_1^+ \to 6_1^+$	209(18)	251.19

In addition to the energy levels, we have calculated the $B(\mathrm{E2})$ transition strengths for some low-lying states of the ground-state bands of these isotopes. To do that, we employed the E2 transition operator, written in the ECQF formalism as

$$\hat{T}(\mathrm{E2}) = e_B \hat{Q}^\chi \cdot \hat{Q}^\chi \,, \tag{4}$$

where $\hat{Q}^{\chi}$ is the quadrupole boson creation operator of Eq. (1), and e_B is the effective charge, determined by equating the intrinsic quadrupole deformation parameter $\beta_t(0_1^+ \to 2_1^+)$ of the IBM-1 model to the $\beta_F^{\min}$ of the mean-field PEC (see [7] for more details). The results are tabulated and compared with available literature data in Table 1, showing reasonable agreement.

4. Summary and outlook

In summary, this contribution presented a sketch of the method detailed in [7], aiming to introduce triaxiality in the classical limit of IBM-1, using only one- and two-body terms, by taking advantage of the proxy-SU(3) approximation to the shell model. This method can provide a quick and easy tool for the calculation of energy spectra and B(E2) transition strengths for many medium-heavy and heavy nuclei, extending IBM predictions to experimentally unexplored regions of the nuclear chart. Current and future research steps involve its application to neighboring isotopic chains (*e.g.* Er, Yb, Os), possibly taking into account the next highest weight irreps of proxy-SU(3) in the derivation of $\gamma_{\rm s}$ [29, 30].

REFERENCES

[1] A.S. Davydov, G.F. Filippov, *Nucl. Phys.* **8**, 237 (1958).
[2] A.S. Davydov, V.S. Rostovsky, *Nucl. Phys.* **12**, 58 (1959).
[3] J. Meyer-ter-Vehn, *Nucl. Phys. A* **249**, 111 (1975).
[4] Y. Tsunoda, T. Otsuka, *Phys. Rev. C* **103**, L021303 (2021).
[5] T. Otsuka *et al.*, arXiv:2303.11299 [nucl-th].
[6] S. Rouoof *et al.*, *Eur. Phys. J. A* **60**, 40 (2024).
[7] P. Vasileiou, D. Bonatsos, T.J. Mertzimekis, *Phys. Rev. C* **110**, 014313 (2024).
[8] F. Iachello, A. Arima, «The Interacting Boson Model», Cambridge Monographs on Mathematical Physics, *Cambridge University Press*, 1987.
[9] J.N. Ginocchio, M.W. Kirson, *Phys. Rev. Lett.* **44**, 1744 (1980).
[10] A.E.L. Dieperink, O. Scholten, F. Iachello, *Phys. Rev. Lett.* **44**, 1747 (1980).
[11] D. Bonatsos *et al.*, *Phys. Rev. C* **95**, 064325 (2017).
[12] D. Bonatsos *et al.*, *Phys. Rev. C* **95**, 064326 (2017).
[13] D. Bonatsos *et al.*, *Symmetry* **15**, 169 (2023).
[14] K. Nomura, N. Shimizu, T. Otsuka, *Phys. Rev. Lett.* **101**, 142501 (2008).
[15] K. Nomura, N. Shimizu, T. Otsuka, *Phys. Rev. C* **81**, 044307 (2010).
[16] K. Nomura, T. Otsuka, N. Shimizu, L. Guo, *Phys. Rev. C* **83**, 041302(R) (2011).

[17] P.-G. Reinhard, B. Schuetrumpf, J. Maruhn, *Comput. Phys. Commun.* **258**, 107603 (2021).

[18] P. Klüpfel, P.-G. Reinhard, T.J. Bürvenich, J.A. Maruhn, *Phys. Rev. C* **79**, 034310 (2009).

[19] E.A. McCutchan, D. Bonatsos, N.V. Zamfir, *Phys. Rev. C* **74**, 034306 (2006).

[20] O. Castaños, J.P. Draayer, Y. Leschber, *Z. Phys. A* **329**, 33 (1988).

[21] J.P. Draayer, S.C. Park, O. Castaños, *Phys. Rev. Lett.* **62**, 20 (1989).

[22] R. Casperson, *Comput. Phys. Commun.* **183**, 1029 (2012).

[23] R.V. Jolos, P. von Brentano, A. Dewald, N. Pietralla, *Phys. Rev. C* **72**, 024310 (2005).

[24] R.V. Jolos, P. von Brentano, *Phys. Rev. C* **74**, 064307 (2006).

[25] R.V. Jolos, P. von Brentano, *Phys. Rev. C* **76**, 024309 (2007).

[26] B. Pritychenko, M. Birch, B. Singh, M. Horoi, *At. Data Nucl. Data Tables* **107**, 1 (2016); *Erratum ibid.* **114**, 371 (2017).

[27] National Nuclear Data Center, `https://www.nndc.bnl.gov/nudat3`

[28] J. Wiederhold *et al.*, *Phys. Rev. C* **99**, 024316 (2019).

[29] D. Bonatsos *et al.*, *J. Phys. G: Nucl. Part. Phys.* **52**, 015102 (2024).

[30] D. Bonatsos *et al.*, *Symmetry* **16**, 1625 (2024).